

## Design and efficiency correlation of IR light-emitting diodes based on quantum dimensional heterostructures AlGaAs

© A.V. Malevskaya, N.A. Kalyuzhnyy, D.A. Malevskii, P.V. Pokrovskii, V.M. Andreev

Ioffe Institute,  
194021 St. Petersburg, Russia  
e-mail: amalevskaya@mail.ioffe.ru

Received October 11, 2023  
Revised December 28, 2023  
Accepted January 17, 2024

Investigation of infra-red (850 nm) light-emitting diodes based on AlGaAs quantum dimensional heterostructures, grown by the MOCVD technique, with multiple quantum wells in active region and with internal reflectors: Bragg reflector, additional „reflective“ layer  $\text{Al}_{0.9}\text{Ga}_{0.1}\text{As}$  or back silver mirror, was carried out. Two types of post-growth technology: LED manufacturing planar technology on growth substrate  $n\text{-GaAs}$  and „transfer“ technology of grown heterostructure on carrier-substrate  $p\text{-GaAs}$  and following etching of growth substrate, were investigated. Maximum external quantum efficiency ( $\text{EQE} > 37\%$ ) at current 0.1–0.2 A was achieved in LED based on heterostructure with Bragg reflector and additional Ag-mirror, built-in LED by heterostructure „transfer“ method on  $p\text{-GaAs}$  carrier with the use of argentum paste. Maximum optical power ( $P_{\text{opt}} = 275 \text{ mW}$ ) at current  $I = 1.2 \text{ A}$  was achieved in LEDs, manufactured by „transfer“ method with the use of Au + In alloy.

**Keywords:** light-emitting diode, AlGaAs/GaAs heterostructure, Bragg reflector, quantum wells.

DOI: 10.61011/JTF.2024.04.57534.261-23

### Introduction

The main cause of a low value of external quantum yield in infrared (IR) (850 nm) light emitting diodes (LEDs) based on quantum-dimensional AlGaAs heterostructures grown on GaAs substrate is absorption of electroluminescent radiation in the substrate. Increase of external quantum yield is possible in case of development of LEDs structures with built-in rear reflectors and removed growth substrate. In such a structure electroluminescent radiation falling onto light yielding surface at the higher angles than the limit angle of full internal reflection is not absorbed inside the structure, as well as contributes into the radiation yielding from the structure. The processes contributing into the radiation yield from the structure are either light reflection from the rear surface of the structure or absorption and secondary radiation of photons in the material of active region. Thanks to these effects multipass light emitting heterostructures allow to considerably increase the external quantum yield of radiation.

Initially, multipass LEDs were manufactured by liquid-phase epitaxy [1–4] with further removal of GaAs growth substrate. Significant disadvantage of such LEDs is that high values of external quantum yield were obtained at high densities of current  $j > 10^2 \text{ A/cm}^2$ , as a result of slow increase of internal quantum yield of emitting recombination as far as the current is increased. Main cause of such smooth dependence of the internal quantum yield with the current increase is a relatively high thickness (over  $1 \mu\text{m}$ ) of narrow-bandgap active region, where saturation of radiation-

free recombination channels was achieved only at current densities  $j > 10^2 \text{ A/cm}^2$ .

Considerably lower thickness of active region is embodied in LEDs based on quantum-dimensional heterostructures produced by MOC-hydride epitaxy [5,6]. In such LEDs achievement of maximum values of internal and external quantum yield is provided at the current densities of lower than  $10 \text{ A/cm}^2$  [5–7].

Reduction of internal optical losses of electroluminescent radiation (due to absorption in the substrate) in LEDs based on MOC-hydride quantum-dimensional heterostructures was achieved either by removal (selective etching off) of the substrate after growing the heterostructure [6], or by creation of an internal Bragg reflector between GaAs-substrate and  $p\text{-}n$ -junction [7].

This paper presents the results of the study of IR (850 nm) LED based on AlGaAs/GaAs-heterostructures produced by MOC-hydride epitaxy, with multiple quantum wells within the active region, with rear Bragg reflector, with reflecting layer of  $\text{Al}_{0.9}\text{Ga}_{0.1}\text{As}$  and with rear silver mirror.

### 1. Production of heterostructures for LEDs

AlGaAs/GaAs-heterostructures were grown on  $n\text{-GaAs}$  substrates (Fig. 1). Active region between wide-band layers consists of 6 pairs of InGaAs layers of quantum wells with the thickness of 3 nm each, divided by  $\text{Al}_{0.2}\text{Ga}_{0.8}\text{As}$ -layers with the thickness of 30 nm each [6]. Active region with the total thickness of  $0.2 \mu\text{m}$  on both sides

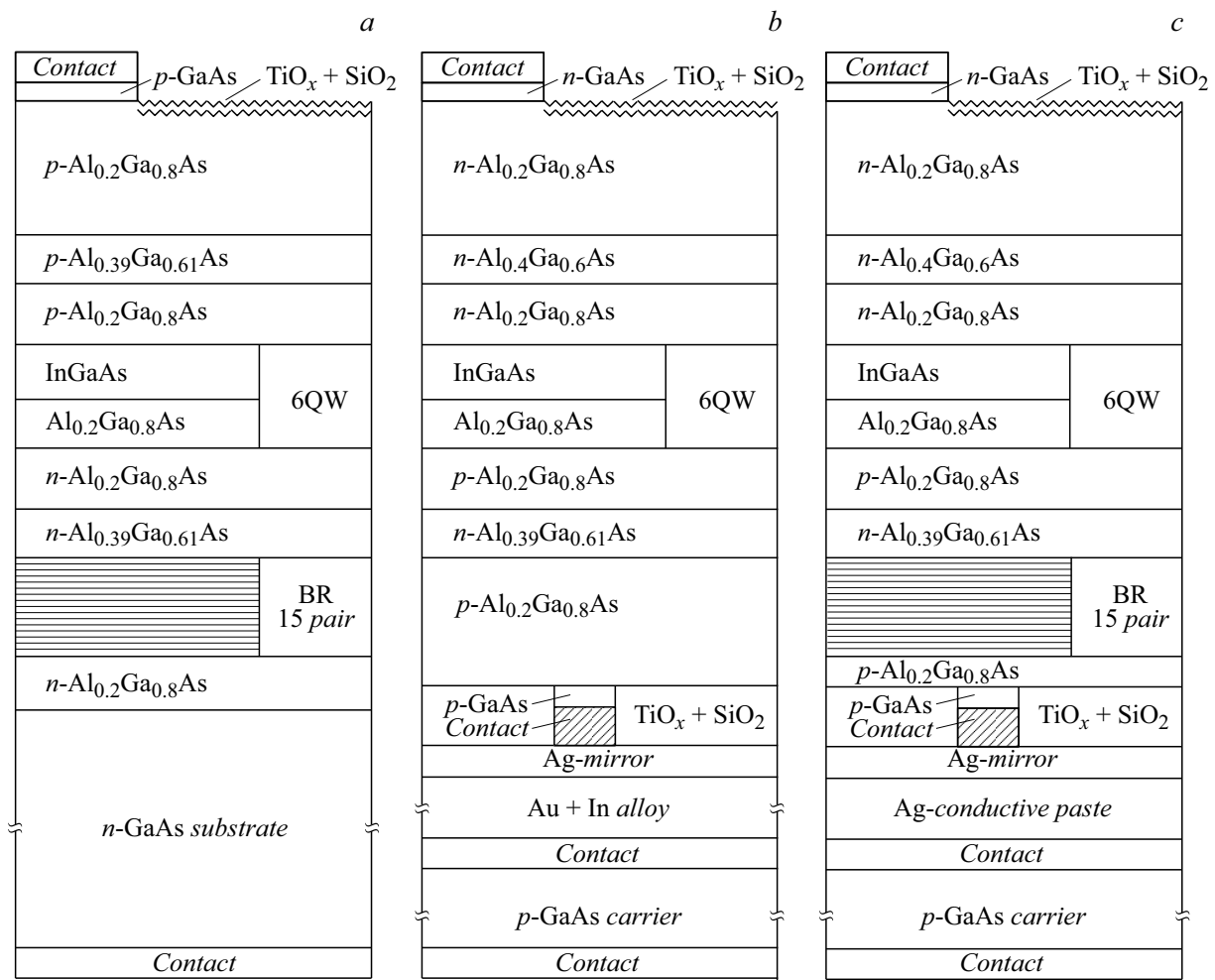


**Figure 1.** Three studied structures of IR (850 nm) LEDs: *a* — „direct“ structure with rear Bragg reflector and additional reflecting layer  $n\text{-Al}_{0.9}\text{Ga}_{0.1}\text{As}$ ; *b* — „inverse“ structure of LED with rear mirror layer of silver; *c* — „inverse“ structure of LED with Bragg reflector added by Ag-mirror.

is placed among cladding of  $n$ - and  $p$ -types formed by the pairs of wide-band layers  $\text{Al}_{0.2}\text{Ga}_{0.8}\text{As}$  ( $0.6\ \mu\text{m}$ ) and  $\text{Al}_{0.4}\text{Ga}_{0.6}\text{As}$  ( $0.36\ \mu\text{m}$ ).

In the structure given in Fig. 1, *a*, the layers of rear combined reflector were grown between  $n\text{-GaAs}$  substrate and active region with cladding: the first layer  $n\text{-Al}_{0.9}\text{Ga}_{0.1}\text{As}$  providing reflection from heteroboundary of „lateral“ beams propagating from  $p$ - $n$ -junction towards the substrate at the angles exceeding the limit angle of full internal reflection ( $\sim 60^\circ$ ), which would be absorbed in the substrate in the absence of that „reflecting“ layer  $\text{Al}_{0.9}\text{Ga}_{0.1}\text{As}$ .

Then the layers of Bragg reflector were crystallized, including 15 pairs of  $n\text{-Al}_{0.9}\text{Ga}_{0.1}\text{As}/n\text{-Al}_{0.1}\text{Ga}_{0.9}\text{As}$  layers, reflecting the beams in solid angle with the aperture  $\pm 20^\circ$ .

Once the active region layers are grown, a heavily-doped  $p^+\text{-Al}_{0.2}\text{Ga}_{0.8}\text{As}$  layer was crystallized ( $5\ \mu\text{m}$ ). The growing of heterostructure was completed by crystallization of a heavily-doped thin ( $0.1\ \mu\text{m}$ ) „contact“ layer  $p^+\text{-GaAs}$ , to be etched off at the contact-free locations. The considered

structure will hereinafter referred to as the „direct“ structure as opposed to two „inverse“ structures discussed below.

„Inverse“ structure shown in Fig. 1, *b* was also grown on  $n\text{-GaAs}$  substrate, however the sequence of layers is inverse versus „direct“ structure discussed above. First,  $\text{Al}_{0.9}\text{Ga}_{0.1}\text{As}$  layer was crystallized, used as the „stop“-layer in case of etching off the  $n\text{-GaAs}$  growth substrate in the process of post-growth transfer of heterostructure onto a carrier substrate ( $p\text{-GaAs}$ ) and completely etched off after the substrate removal. Next,  $n\text{-GaAs}$  contact layer was crystallized. Next,  $n\text{-Al}_{0.2}\text{Ga}_{0.8}\text{As}$  layer was crystallized with the thickness of  $4\ \mu\text{m}$ , as shown in the top part of Fig. 1, *b*. Then, the layers of active region and cladding were grown, the same as shown in Fig. 1, *a*. After that,  $p\text{-Al}_{0.2}\text{Ga}_{0.8}\text{As}$  buffer layer was crystallized and a thin ( $0.1\ \mu\text{m}$ )  $p\text{-GaAs}$  contact layer for deposition of „point“ contacts.

The difference of the „inverse“ structure shown in Fig. 1, *c*, from the structure in Fig. 1, *b* refers to an additional Bragg reflector crystallized between the active region with cladding and „buffer“ layer of  $p\text{-Al}_{0.2}\text{Ga}_{0.8}\text{As}$ .

## 2. Post-growth technologies of LED manufacture

When manufacturing LEDs based on „direct“ structure, frontal bus-bar ohmic contact to GaAs *p*-type conductivity layer was formed by deposition of Ag(Mn)/Ni/Au layers with the thickness of 0.2–0.3 μm, with specific contact resistivity  $(3–5) \cdot 10^{-5} \Omega \cdot \text{cm}^2$ . In order to increase conductivity of contact bus-bars Ag/Ni/Au layers with the thickness of 2–4 μm were electrochemically deposited. In Fig. 2 the top left detail shows topology of contact grid of LED with the area of 1 mm<sup>2</sup>.

In order to increase efficiency of the radiation yield from the crystal, the frontal light yielding surface of LED was textured.

Rear ohmic contact to GaAs substrate of *n*-type conductivity was formed based on the Au(Ge)/Ni/Au layers, with specific contact resistivity  $(1–2) \cdot 10^{-6} \Omega \cdot \text{cm}^2$ . In order to increase efficiency of light yield from the LED crystal, silicon hemisphere was formed on its light yielding surface.

The post-growth technology of LEDs production based on „inverse“ structures is described below. At first, point contacts ( $\varnothing 10 \mu\text{m}$ , spacing 75 μm) to the *p*<sup>+</sup>-GaAs contact layer were created on the surface of grown heterostructure. Then, selective removal of *p*-GaAs contact layer was performed in contact-free locations, with further deposition of dielectric coatings TiO<sub>x</sub>/SiO<sub>2</sub> for protection of the semiconductor surface against direct contact with the layer of silver mirror, which is deposited next onto dielectric coating. The dielectric coating also performs the function of additional layer of reflector providing reflection of beams falling onto it at higher angles than the angle of full internal reflection, from the dielectric–semiconductor boundary.

Transfer of AlGaAs/GaAs-heterostructure onto GaAs-substrate–carrier was performed with the use of silver-containing paste (Ag-paste) (Fig. 1, *c*) or Au–In-alloy (Fig. 1, *b*). The use of Ag-paste does not allow to form a low-resistance connection of the heterostructure and the substrate–carrier, which leads to significant ohmic losses in case of increase of the operating current. Transfer of heterostructure onto substrates–carriers with the use of gold-indium alloy leads to formation of crystalline Au–In intermetallic compound, which provides reduction of serial resistance of LED.

Final stages of the structures manufacture: removal of *n*-GaAs growth substrate in a selective etcher; manufacture of bus-bar contacts; removal of *p*-GaAs contact layers in contact-free locations; texturing of light yielding surface; deposition of antireflection coating TiO<sub>x</sub> + SiO<sub>2</sub>.

Therefore, three types of LEDs with similar active regions differing in the structure of rear reflectors were manufactured.

The 1st type of LED (Fig. 1, *a*) was made on the basis of „direct“ structure with Bragg reflector providing reflection of beams in a solid angle with aperture  $\pm 20^\circ$ , and with additional Al<sub>0.9</sub>Ga<sub>0.1</sub>As layer that provides lateral beams

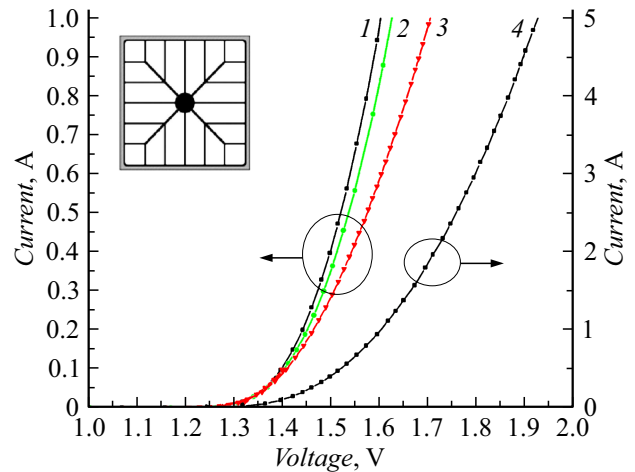


**Figure 2.** Current-voltage curve and topology of LEDs based on structures shown in Fig. 1: curves 1, 2, 4 — LEDs based on „direct“ structure (Fig. 1, *a*); 3 — LEDs with rear Ag-mirror based on the structure shown in Fig. 1, *b*, whose transfer onto a *p*-GaAs carrier substrate was performed by using Au + In alloy.

falling onto the heteroboundary at higher angles than the limit angle of full internal reflection.

The 2nd type of LED (Fig. 1, *b*) was made on the basis of „inverse“ heterostructure with rear Ag-mirror made by heterostructure transfer onto *p*-GaAs carrier with the use of Au + In-alloy.

The 3rd type of the structure (Fig. 1, *c*) differs from the 2nd type by the presence of Bragg reflector and the heterostructure transfer onto the carrier performed by using a silver-containing paste.

## 3. Study of LED characteristics

Measurements of current-voltage curve (CVC) and watt-ampere characteristics of LEDs (Fig. 2) were performed as follows: current pulses with constant amplitude were applied through the studied sample ( $\tau_{\text{imp}} = 5–300 \mu\text{s}$ ), voltage was registered, LED radiation was absorbed by a control photodetector with known spectral dependence of photosensitivity ( $SR_{\text{pd}}, \text{A/W}$ ), photodetector current was registered ( $I_{\text{pd}}, \text{A}$ ), optical power of LED was calculated:  $P_{\text{opt}} = I_{\text{pd}}/SR_{\text{pd}}, \text{W}$ .

Current dependences of external quantum efficiency ( $\eta_{\text{ext}}$ ) [8], defined as the relationship between the quantity of radiation quanta from the LED ( $N_{\text{hv}} = P_{\text{opt}}/h\nu$ ) and the number of injected electrons ( $N_e = I/e$ ), were calculated by using measured watt-ampere characteristics:  $\eta_{\text{ext}} = P_{\text{opt}}e/h\nu \cdot I$ , where  $P_{\text{opt}}$  — optical power of LED,  $I$  — LED current,  $h\nu$  — energy of emitted quanta and  $e$  — electron charge.

With the currents up to 1–5 A and the area of chips 1 mm<sup>2</sup> the pulse mode enabled testing up to the current densities of 100–500 A/cm<sup>2</sup> in the developed LEDs

mounted onto bases made of metallized alumo-oxide heat conducting electric insulating ceramics.

Current-voltage curves shown as curves 1, 4 in Fig. 2 were measured for LEDs produced on the basis of a „direct“ structure, with the central contact spot with the diameter of  $150\mu\text{m}$  deposited directly onto the contact layer of  $p\text{-GaAs}$ . CVC shown as the curve 2 in Fig. 2 was obtained for LEDs when making which the central contact spot was deposited onto additional layer of dielectric with the diameter of  $130\mu\text{m}$ , which was deposited in order to prevent the current flowing directly beneath that contact spot for the sake of reducing optical losses due to radiation absorption by the contact layer. However, an increase of serial resistance of LED with the dielectric sublayer, as found in CVC (Fig. 2, the curve 2) and deterioration of adhesion of contact layer of metal to dielectric, and, as a consequence, decrease of the efficiency factor, forced us to refuse of the deposition of an additional layer of dielectric under the central contact spot.

The measured values of serial LED resistance with the area of  $1\text{mm}^2$  were  $R = 0.08\Omega$  in LEDs based on „direct“ structure. The resistance  $R = 0.16\Omega$  was measured (curve 3 in Fig. 2) in LEDs obtained by transfer of „direct“ structure onto the  $p\text{-GaAs}$  carrier by using Au + In-alloy. Increase of the resistance several times and the spread of its values were observed in LEDs with transfer of inverse structure performed by using Ag-paste.

Optical power  $P$  in the studied LEDs was:

- In LEDs based on „direct“ structure  $P = 190\text{mW}$  at the current of  $I = 1.5\text{A}$  (Fig. 3, curve 1);
- In LEDs obtained by transfer of heterostructure onto a carrier by using Au + In-alloy, the optical power was  $P = 250\text{mW}$  at the current  $I = 1\text{A}$  (Fig. 3, curve 2) and  $P = 275\text{mW}$  at the current  $I = 1.2\text{A}$ ;

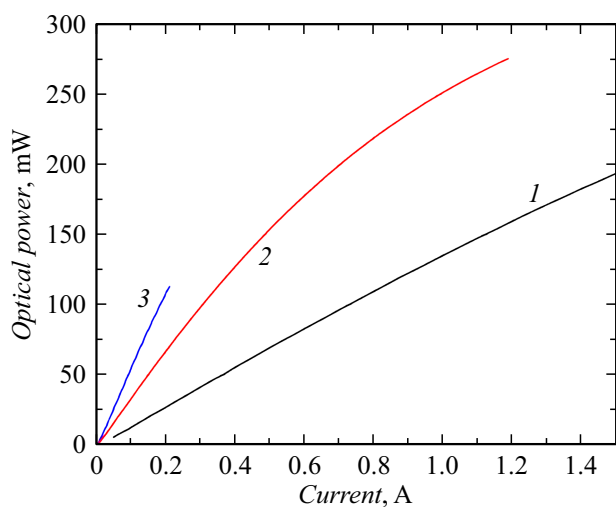


**Figure 3.** Watt-ampere characteristics of LEDs: 1 — LEDs based on „direct“ heterostructure; 2 — LEDs based on „inverse“ heterostructure with rear Ag-mirror; 3 — LEDs based on the structure with Bragg reflector and rear Ag-mirror.

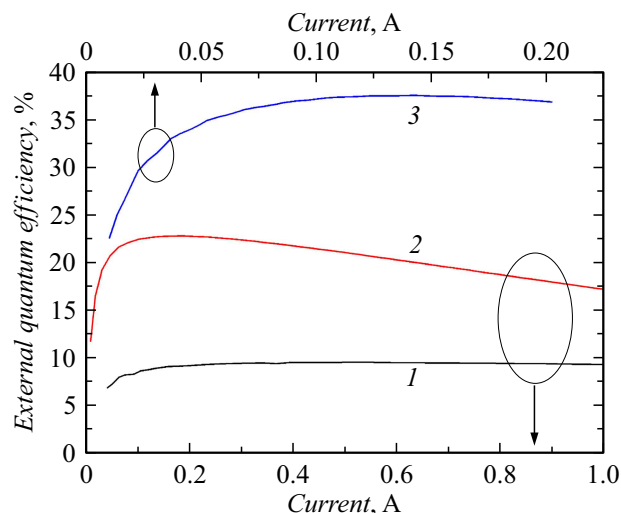


**Figure 4.** Current dependencies of the external quantum efficiency: 1 — LEDs based on „direct“ structure; 2 — LEDs with rear Ag-mirror and with Au + In eutectics; 3 — LEDs with Ag-mirror, with Bragg reflector added by Ag-mirror, and with Ag-paste.

- in LEDs obtained by transfer with the use of Ag-paste  $P = 110\text{mW}$  at the current  $I = 0.2\text{A}$  (Fig. 3, curve 3).

Therefore, the maximum power was obtained in LEDs made by „transfer“ with the use of Au + In-alloy.

The values of external quantum efficiency in these LEDs were (Fig. 4):

- 9–9.5% within the range of currents 0.2–1 A in LEDs based on „direct“ structure (curve 1 in Fig. 4);
- 23% at the current of 0.2 A and 17% at the current 1 A (curve 2 in Fig. 4) in LEDs based on the structure with Ag-mirror produced by transfer of heterostructure onto a carrier with the use of Au + In alloy;
- 37% within the range of currents 0.1–0.2 A (curve 3 in Fig. 4) were obtained in LEDs based on the structure with Ag-mirror and Bragg reflector produced by transfer of heterostructure onto a carrier with the use of Ag-paste.

According to the results of CVC measurements and watt-ampere characteristics of LEDs, the following conclusions can be made:

Maximum value of external quantum efficiency is achieved in LEDs based on the structure with Bragg reflector and a rear silver mirror built-into the structure. At the same time, decrease of internal resistance and increase of LEDs power is achieved by replacing Ag-paste with an interlayer of Au + In-alloy in the technology of heterostructure transfer from the growth  $n\text{-GaAs}$ -substrate onto a carrier substrate  $p\text{-GaAs}$ .

## Conclusion

The studies of impact of the structures and technologies of IR (850 nm) LEDs based on quantum-dimensional heterostructures with Bragg reflector in combination with

rear „reflecting“ layer  $\text{Al}_{0.9}\text{Ga}_{0.1}\text{As}$ , as well as of LEDs with Bragg reflector and Ag-mirror produced by transfer of AlGaAs-heterostructure onto a carrier substrate with further growth substrate etching off were performed.

The maximum external quantum efficiency over 37% within the range of current 0.1–0.2 A was obtained in LEDs with rear Bragg reflector and Ag-mirror manufactured by „transfer“ technology with the use of silver-containing paste. Maximum values of optical power  $P = 275$  mW at the current of 1.2 A were obtained in LED manufactured by transfer of heterostructure onto a carrier with the use of Au + In-alloy.

Its own application niche can be defined for every type of the studied LEDs. Low-area LEDs based on „direct“ structure with combined internal reflector, manufactured by a simple planar post-growth technology, could be applied in optoelectronic integral VHF circuits.

High-efficiency LEDs manufactured by the „transfer“ technology with the use of Ag-paste could be applied in low-power ( $P < 100$  mW) optoelectronic devices.

Highly efficient powerful LEDs ( $P > 250$  mW), manufactured by „transfer“ with the use of Au + In-alloy could be widely applied, e.g. for background IR light and in security systems.

Regarding the perspectives of IR LEDs efficiency improvement. One of the ways to resolve that problem is creation of a two-section Bragg reflector, whose first section provides reflection of beams within the solid angle from the normal line to  $30^\circ$ , and the second section manufactured with 1.3 times (approximately) increased period of pairs of  $\text{Al}_{0.9}\text{Ga}_{0.1}\text{As}/\text{Al}_{0.1}\text{Ga}_{0.9}\text{As}$  layers will provide reflection of beams within the solid angle with the aperture  $30\text{--}60^\circ$  relative to the normal line to heteroboundaries. This range of angles is a „black hole“ (without the second section) absorbing electroluminescent radiation not reflected by both the first section of Bragg reflector, and the radiation not reflected from the heteroboundary with the  $\text{Al}_{0.9}\text{Ga}_{0.1}\text{As}$  layer, reflecting lateral layers with the incidence angles of  $60\text{--}90^\circ$  to the normal line, which exceed the limit angle of full internal reflection. Therefore, the second section of two-section Bragg reflector could „close“ that „black hole“ and ensure reduction of optical losses.

Implementation of that structure of two-section Bragg reflector in combination with  $\text{Al}_{0.9}\text{Ga}_{0.1}\text{As}$  reflective layer and Ag-mirror should ensure significant increment of the LEDs efficiency.

## Acknowledgments

The authors thank M.Z. Shvarts, N.D. Il'inskaya, S.A. Mintairov, R.A. Saliy, Yu.M. Zadiranov, N.S. Potapovich, F.Yu. Soldatenkov and R.V. Levin for the help and consultancies during performance of experiments.

## Conflict of interest

The authors declare that they have no conflict of interest.

## References

- [1] Zh.I. Alferov, V.M. Andreev, D.Z. Garbuzov, N.Yu. Davidyuk, B.V. Egorov, B.V. Pushnyi, L.T. Chichua. *ZhTF*, **48** (4), 809 (1978).
- [2] A.L. Zakgeim, V.M. Marakhonov, R.P. Seisyan. *Pis'ma v ZhTF*, **6** (17), 1034 (1980) (in Russian).
- [3] U. Bekirev, S. Babenko, V. Krykov, B. Potapov, A. Skiper. *Elektronika*, **00137**, 137 (2014) (in Russian).
- [4] Electronic source. *AO AO Nauchno-Issledovatel'skii Institut Poluprovodnikovyykh Priborov*. Access mode: <https://www.niipp.ru/>
- [5] Patent US20230335681A1 dated 10/19/2023.
- [6] A.V. Malevskaya, N.A. Kalyuzhnyy, D.A. Malevskii, S.A. Mintairov, A.M. Nadtochiy, M.V. Nakhimovich, F.Y. Soldatenkov, M.Z. Shvarts, V.M. Andreev. *FTP*, **55** (8), 699 (2021) (in Russian). DOI: 10.1134/S1063782621080121
- [7] Su-Chang Ahn, Byung-Teak Lee, Won-Chan An, Dae-Kwang Kim, In-Kyu Jang, Jin-Su So, Hyung-Joo Lee. *J. Korean Phys. Society*, **69** (1), 91 (2016).
- [8] E.F. Schubert, *Light-Emitting Diodes*, 2<sup>nd</sup> ed., Gambridge University Press (2006).

*Translated by D.Kondaurov*